REPORT DOCUMENTATION PAGE

AFRL-SR-AR-TR-02-

0396

1. AGENCY USE ONLY *(Leave blank)*

2. REPORT DATE
31 Oct 02

3. REPORT TYPE AND DATES COVERED
FINAL REPORT 01 SEP 96 TO 30 SEP 01

4. TITLE AND SUBTITLE
THEORETICAL MODELING OF DAMAGE MECHANISMS FOR ULTRASHORT LASER PULSES IN OCULAR MEDIA

5. FUNDING NUMBERS
F49620-96-1-0438
61102F
2312/AX

6. AUTHOR(S)
Prof. Bernard Gerstman

7. PERFORMING ORGANIZATION NAME(S) AND ADDRESS(ES)
Florida International University
Department of Physics
University Park
Miami, FL 33158

8. PERFORMING ORGANIZATION REPORT NUMBER

9. SPONSORING/MONITORING AGENCY NAME(S) AND ADDRESS(ES)
AFOSR/NL
4015 Wilson Blvd. Room 713
Arlington, VA 22203-1954

10. SPONSORING/MONITORING AGENCY REPORT NUMBER

11. SUPPLEMENTARY NOTES

12a. DISTRIBUTION AVAILABILITY STATEMENT
Approve for Public Release; Distribution Unlimited

12b. DISTRIBUTION CODE

13. ABSTRACT *(Maximum 200 words)*

The funding provided in this grant has allowed the development of a comprehensive computational model for predicting the effect that any laser pulse will have on any spherical absorbing particle. This model is based upon fundamental principles and therefore is capable of determining all thermomechanical responses (temperature rise, shock wave, explosive vaporization) and is applicable to a wide range of materials with unprecedented accuracy. This allows the assessment of potential damage to a variety of materials, such as biological tissue. The computational model is also applicable for investigating and predicting laser induced damage in synthetic polymers and optical and electronic communication materials. The research also furnishes a technique for determining thermomechanical properties of microparticles used in novel medical, biological and material science applications. In addition, we have seen evidence that the thermomechanical response in various materials to a laser pulse is not only non-linear, but chaotic. This implies that small changes in laser pulse characteristics such as duration or energy may lead to enormous changes in response that are extremely damaging to the material whether biological or synthetic. The detailed nature of the investigation and resulting model allowed for the discovery of this chaotic behavior, which had not been previously reported by any other investigators.

14. SUBJECT TERMS

20021126 066

15. NUMBER OF PAGES

16. PRICE CODE

17. SECURITY CLASSIFICATION OF REPORT	18. SECURITY CLASSIFICATION OF THIS PAGE	19. SECURITY CLASSIFICATION OF ABSTRACT	20. LIMITATION OF ABSTRACT
Unclas	Unclas	Unclas	

AFOSR Final Progress Report

1. Period Covered: October 1, 1996 to September 30, 2001.

2. Title: Theoretical Modeling of Damage Mechanisms for Ultrashort Laser Pulses in Ocular Media

3. Grant Number: F49620-96-1-0438

4. Florida International University

5. Prof. Bernard Gerstman
Department of Physics
Florida International University
University Park
Miami, FL 33158

Telephone: 305-348-3115
Fax: 305-348-6700
E-mail: gerstman@biophys.fiu.edu

6.Manuscripts

B. S. Gerstman
"Nanosecond Laser Pulses: Refined Surgical Treatment of Congenital Nevi and Melanoma",
Proceedings of the SPIE, vol. **2975**, 180-191, 1997.

J. Sun and B. S. Gerstman
"Pressure Generation in Melanosomes by Sub-Nanosecond Laser Pulses"
Proceedings of the SPIE, vol. **3254**, 156-167, 1998.

B. S. Gerstman
"Activated Rate Processes and a Specific Biochemical Mechanism for Explaining Laser Induced Thermal Damage to the Retina",
Experimental Eye Research, vol. **67**, suppl. 1, 1998.

J. Sun and B. S. Gerstman
"Modeling of Pressure Generation by Lasers in Melanosomes: How to Avoid Stress Confinement and Blow Up a Melanosome"
Proceedings of the SPIE, vol. **3601**, 43-54, 1999.

B. S. Gerstman
"Theoretical Modeling of Laser-Induced Explosive Pressure Generation and Vaporization in Pigmented Cells",
Proceedings of the 31st Annual Boulder Colorado Damage Symposium, Laser-Induced Damage in Optical Materials: 1999; Editors: G. J. Exarhos, A. H. Guenther, M. R. Kozlowski, K. L. Lewis, M. J. Soileau, Proceedings of SPIE, vol. **3902**, 41-53, 2000.

J. Sun, B. S. Gerstman, B. Li

"Shock Wave Generation and Bubble Formation in the Retina By Lasers",
Proceedings of SPIE, vol. **3914**, 154-165, 2000.

J. Sun and B. Gerstman,
"Photoacoustic Generation for a Spherical Absorber with Impedance Mismatch with the Surrounding Media",
Physical Review E, vol. **59(5)**, 5772-5789, 1999.

B. S. Gerstman and J. Sun,
"Laser-induced retinal shock waves and bubbles and their dependencies on the thermomechanical properties of melanosomes",
Proceedings of SPIE, vol. **4257**, 149-158, 2001.

J. M. Sun, B. S. Gerstman, and B. Li,
"Bubble dynamics and shock waves generated by laser absorption of a photoacoustic sphere",
Journal of Applied Physics, vol. **88**(5), 2352-2362, 2001.

"Chaotic turbulence in a photoacoustic spherical system",
J. M. Sun and B. S. Gerstman,
submitted, Physical Review Letters.

7. Scientific Personnel supported by grant:

Prof. Bernard Gerstman, Principal Investigator, supported only during summer;
Dr. Jinmimg Sun, Post-Doctoral Research Associate
Graduate Students:

Bin Li
Shijun Wang

8.Discoveries (Please see Item 11 for more detailed explanations.):
i. Laser pulse duration "Stress Confinement" is not valid for limiting the tensile stresses created at the core of an absorber. Therefore, the same laser becomes increasingly more dangerous as pulse lengths are shortened without limit.

ii.Chaotic responses of biological and synthetic materials resulting from laser absorption, leading to windows of pulse characteristics (duration, energy) that present unanticipated danger, or safety.

9. Collaborators:

10: Honors
Prof. Gerstman has been invited to speak on this research at numerous major institutions and conferences and has also been asked to Chair sessions:
AFOSR Ultrashort Laser Workshops
The United States Food and Drug Administration
Harvard University
Laser Bioeffects Meeting, Paris

University of Virginia
Laser Bioeffect Meetings, Baltimore
International Conference on Laser Optics, St. Petersburg, Russia, June 2000.
The International Society for Optical Engineering
Annual Boulder Damage Symposium

11. Key Findings/Results/Accomplishments

The funding provided in this grant has allowed the development of a comprehensive computational model for predicting the effect that any laser pulse will have on any spherical absorbing particle. This model is based upon fundamental principles and therefore is capable of determining all thermomechanical responses (temperature rise, shock wave, explosive vaporization) and is applicable to a wide range of materials with unprecedented accuracy. This allows the assessment of potential damage to a variety of materials, such as biological tissue. The computational model is also applicable for investigating and predicting laser induced damage in synthetic polymers and optical and electronic communication materials. The research also furnishes a technique for determining thermomechanical properties of microparticles used in novel medical, biological and material science applications. In addition, we have seen evidence that the thermomechanical response in various materials to a laser pulse is not only non-linear, but chaotic. This implies that small changes in laser pulse characteristics such as duration or energy may lead to enormous changes in response that are extremely damaging to the material whether biological or synthetic. The detailed nature of the investigation and resulting model allowed for the discovery of this chaotic behavior, which had not been previously reported by any other investigators.

11.1. Description of Physical Model

In order to produce a model that had the most powerful predictive capabilities, it was necessary to start with an understanding of the system in terms of the fundamental physics. The model used consists of a uniform solid spherical absorber surrounded by a transparent medium. The rate of energy input per unit mass is given by

$$\dot{I}_e = \frac{3I_o}{4a\tau_o\rho_o}\left[1-\frac{1}{2\alpha_L^2 a^2}\left(1-e^{-2a\alpha_L}(1+2\alpha_L a)\right)\right] \qquad (1)$$

where I_o is the incident laser fluence in *Joule/cm*^{2}, 'a' is the radius of the absorbing sphere, ϑ_o is the laser pulse duration, Δ_o is the static density of the sphere, and $\forall_L$ is the absorption coefficient of the sphere.

In order to solve the equations governing the temperature, pressure, and density of the system, it is useful to distinguish between two coordinate systems. Since the absorber is treated as spherical, both systems are one-dimensional, corresponding to the radial coordinate. The Lagrangian system (r) is a space fixed system that can be used to locate position in the laboratory frame of reference. The Eulerian coordinate (u) is a mass fixed system and represents the position of a unit mass. The position of each unit mass can change as the system responds to the absorption of laser energy, u=u(r,t). Each unit element of mass is denoted by its initial position , u(r,t=0)=r. The calculations for the thermomechanical response of the system can be carried out in Eulerian coordinates, and then converted back into laboratory coordinates for comparison with

experiments. Density fluctuations can occur throughout the system and can be related to the static density Δ_o through conservation of mass

$$\rho_o dV_r = \rho dV \tag{2}$$

where $\rho=\rho(t)$ is the time varying density.

The following equations are the fundamental physical and thermodynamic equations that describe the behavior of the system. In the following equations, the mathematical dot operation $\dot{f}(t)$ means a total time derivative, the spatial derivative Λ is taken with respect to r, while the spatial derivative with respect to u is denoted by Λ_u. With this notation, the equation of motion of a point is

$$\rho \ddot{u} = -\nabla_u P \tag{3}$$

where P is the pressure and $\Delta=\Delta(t)$ is the time varying density. The next equation that is required is an equation of state (EOS) relating P, V, T. If a material undergoes only small changes in density it can be treated as having a bulk modulus B and thermal expansion coefficient $\forall$ that remain constant. The equation of state is this case can be expressed as

$$\frac{\dot{v}}{v} = -\frac{\dot{P}}{B} + \alpha \dot{T} \tag{4}$$

where $v=1/\Delta$ is the specific volume and is related to u by

$$\dot{v} = \frac{\partial v}{\partial t} + \dot{u} \cdot \nabla_u v \tag{5}$$

This allows the EOS to be written as

$$\frac{\dot{v}}{v} = -\frac{\dot{P}}{B} + \alpha \dot{T} = \nabla_u \cdot \dot{u} \tag{6}$$

In order to predict all possible thermomechanical responses of the system, including explosive vaporization and shock waves, large changes in phase and pressure must be considered. If the material undergoes large changes in density or pressure, such as a phase change, the right hand sides of Eqs. (4) and (6) are no longer valid. In this situation, a full EOS of the material is necessary that is valid over the full range of P, V, T, and ρ. This consideration added a significant complication to our research, which we were able to solve, as discussed later.

Energy conservation of the absorber relates the rate of energy absorption to the increase in internal energy versus the heat lost through conduction to the surrounding medium. The rise in internal energy results in a change in the entropy of the material

$$\dot{I}_e = T\dot{s} - \frac{\lambda}{\rho}\nabla_u^2 T \tag{7}$$

where s is the specific entropy, c_v is the specific heat, and 8 is the thermal conductivity of the absorber. If the simple EOS of Eqs. (4) and (6) is valid, then the entropy term can be related directly to changes in v and T

$$\dot{I}_e = c_v \dot{T} + B\alpha T\dot{v} - \frac{\lambda}{\rho}\nabla_u^2 T \tag{8}$$

The right side of Eq. (8) is only valid when the material remains in the same phase with constant B and $\forall$.

Equations (2)-(8) for describing thermodynamic and hydrodynamic behavior can be used for determining the response of both the absorbing particle and the surrounding material. However, as previously explained, phase changes and shock waves require a more complete EOS than used in Eqs. (4), (6), (8). The Principal Investigator carried out two different major investigations based upon different expressions for the EOS of the medium.

11.2. Analytical Solution for the Linearized Model: Exploding Particles (Micron Size Handgrenades)

We first analyzed the system using the EOS of Eq. (4) for both the medium and for the absorber, but with different values of B and α. This EOS, valid only for acoustic pressure waves and small changes in density does not treat phase changes (vaporization) or shock waves in the medium. However, it is valid for investigating strong acoustic waves that can lead to damage in biological systems where the surrounding system is cellular fluid. This analysis is also relevant for solid media such as dielectrics and polymer materials. Another important advantage of the use of this EOS for the medium is that it allows the system to be mathematically linearized and solved analytically. This resulted in a major discovery concerning the explosive stresses on the absorbing particle.

We are treating the system as spherically symmetric which implies that u has no curl and we can therefore write changes in u as the gradient of a scalar function N: $*u=\Lambda N$. The equation of motion, Eq. (3), and the equation of state, Eq. (6), both inside the absorber and outside in the surrounding material can be rewritten as

$$\delta P = -\rho_o \ddot{\phi} \tag{9}$$

and

$$\frac{1}{c^2}\ddot{\phi} = \nabla^2\phi - \alpha\delta T \tag{10}$$

with $c^2=B/\Delta_o$, $*P=P-P(0)$, and $*T=T-T(0)$. Analogous equations are used for the medium. These equations can then be solved in a lengthy and complex procedure by first performing a Laplace transformation on time to define the function

$$M(r,s)=\square[N(r,t)] \tag{11}$$

and then applying a Green's function method on the spatial coordinates. The extended details of this complicated theoretical analysis are given in the paper referenced above that appears in Physical Review E. A result of major importance from this work is that the solution gives analytical, not numerical, expressions that permit the prediction of changes in pressure, density, and temperature both in the absorbing particle and in the surrounding medium.

The following figure, Fig. 1, displays an extremely important result of these calculations. This result can be used to determine potential risk for damage in a variety of materials, as well as for determining mechanical parameters of micro and nano particles that are increasingly used in advanced biomedical and material science techniques.. The figure shows the pressure transients that will be created in the surrounding medium when the absorbing particle and the surrounding medium have different mechanical impedances, due to different densities or bulk moduli. This is

relevant for retinal tissue where the absorbing particles are melanosomes, dielectric materials and polymers with impurities, and gold particles used in biomedical and biophysical manipulations of individual biomolecules such as DNA or proteins. Because of the mismatch in mechanical impedances, the outgoing pressure signal that is generated in the absorber is reflected at the boundary. The reflection travels back to the singularity at the center of the absorber where it is reflected again and becomes a second outgoing pressure signal which trails the first by a time ϑ_c=2a/c, where 'a' is the radius of the absorber and c is the speed of sound in the absorber. The multiple pressure signals due to the reflections create the ringing patterns displayed in Fig. 1. This ringing pattern will exist everywhere, both inside the absorber and outside in the medium where it can damage the surrounding biological tissue or electronic material. Figure 1 displays the pressure at a position r=2a which is outside the absorber, in the medium.

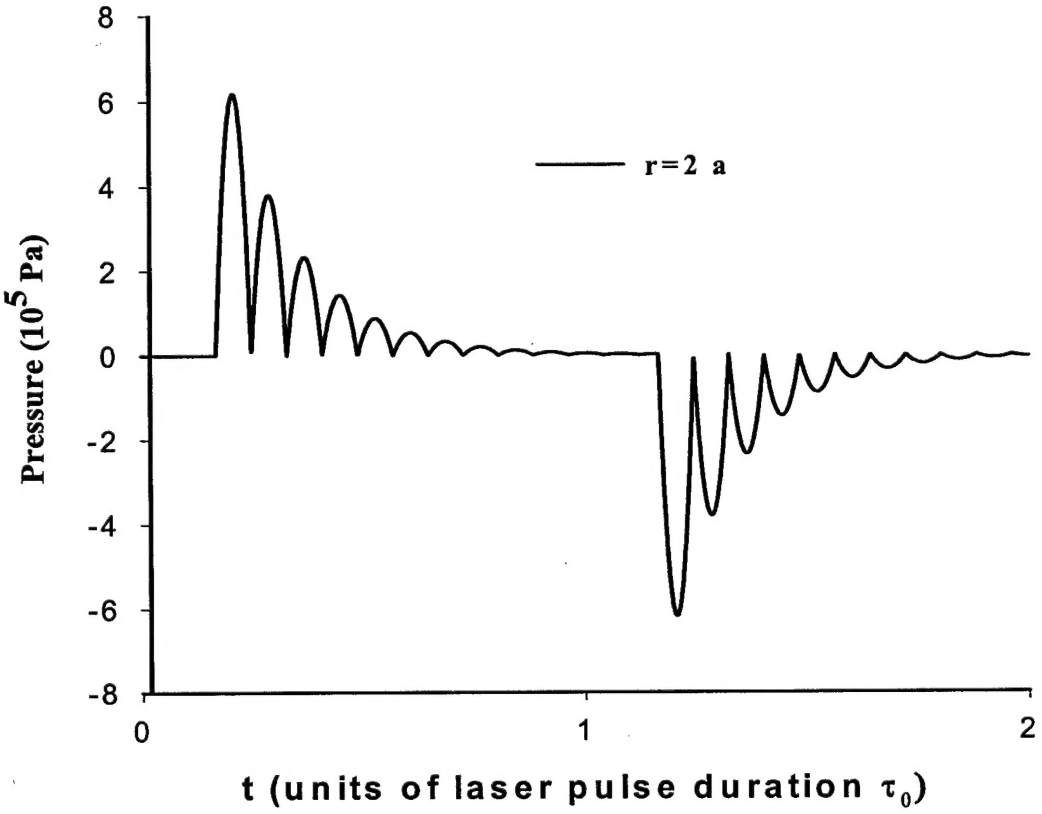

Figure 1

This ringing pattern can be extremely useful for investigating thermo-mechanical properties of the absorber. To accurately predict the strength of shock fronts and the size of bubbles, the model requires values for the bulk modulus and thermal expansion coefficient of the absorber. These values are not known for melanosomes or for many other microparticles of interest. Obtaining values for these parameters by performing measurements directly on the absorber itself is extremely difficult due to the small size of the particle. However, one of the important results from the theoretical work shows how the bulk modulus and thermal expansion coefficient can be determined from measurements on acoustic waves generated in the surrounding medium, which is experimentally possible using laser interferometry.

The pressure signal in the medium (Fig. 1) will have peaks of duration ϑ_c=2a/c, where 'a'

is the radius of the absorber and $c = \sqrt{B/\rho_o}$ is the speed of sound in the absorber. The density of the absorbing particle is relatively easy to determine; for melanosomes it is approximately 1.35 g/cm^3. Therefore, a measurement of ϑ_c will then give a value for the important parameter *B*. The amplitude of the acoustic waves is proportional to both the bulk modulus and the thermal expansion coefficient. Therefore, a measurement of the amplitude of the pressure wave, combined with the previous measurement that gives the bulk modulus, will allow the determination of a value of the thermal expansion coefficient, the other parameter that is necessary for theoretical predictions of shock fronts and bubbles. The same technique can be used to determine the thermo-mechanical properties of any absorbing microparticles and nanoparticles such as polystyrene and gold that are increasingly used in research involving the manipulation of individual molecules, such as DNA.

Another major result of this work is that the concept of a laser pulse confinement time is not valid for the stresses experienced at the core of the absorber. It was postulated that the transit time for acoustic waves across the absorber, ϑ_c=2a/c, would act as a "stress confinement time". This would mean that different laser pulses of the same energy would generate the same pressure responses independent of the duration of the pulses as long as the pulses are all of shorter duration than the stress confinement time ϑ_c. The acoustic speed in melanosomes is not known because of the difficulty in making measurements on micron size particles. Since it is a solid particle it is likely to have an acoustic speed in the range of 10^3-10^4 m/s which gives an acoustic transit time across a micrometer size particle of 10^{-10}-10^{-9} seconds.

Sub-nanosecond laser pulses have been in existence for many years and the power output in picosecond and femtosecond lasers is continually increasing. It is therefore of crucial importance to determine if the concept of stress confinement is valid, which would imply that picosecond and femtosecond pulses are no more dangerous than nanosecond pulses. We determined that this was absolutely *not* true and that the danger continues to increase as the pulse duration is shortened.

Our work established the unexpected result that the tensile stress at the core continued to grow even as the laser pulse duration was made shorter than the acoustic transit time. The amplitude of the maximum tensile pressure varies inversely with the pulse duration

$$|P_{\max}| \propto \frac{1}{\tau_o} \qquad (12)$$

This surprising dependence for $\vartheta_o < \vartheta_c$ is displayed in Fig. 2. The fact that it is the tensile, negative pressure that continues to increase at the core makes the situation especially dangerous. It shows that the same energy delivered in a shorter pulse is increasingly more likely to cause an absorbing particle to explode like a laser-activated handgrenade. Our work shows that this dangerous effect will be present not just for melanosomes in the retina, but for any absorbing particle in any media, and for self-focusing in transparent uniform materials such as water or polymers. In Fig. 2 the absorbing particle has been assigned values of a, B and ρ_o such that the absorber has a transit time τ_c=4x10^{-8} seconds. If the concept of stress confinement of pressure effects is correct, then all laser pulses with τ_o less 40 nsec should produce the same tensile stress at the core. Figure 2 shows that this is not true for pulses with $\tau_o \ll \tau_c$ and therefore stress confinement is not valid. This discovery implies that laser pulses become increasingly more dangerous as the pulse length is shortened and that the continual increase in tensile stress can

cause the absorber to explode at increasingly lower laser energies.

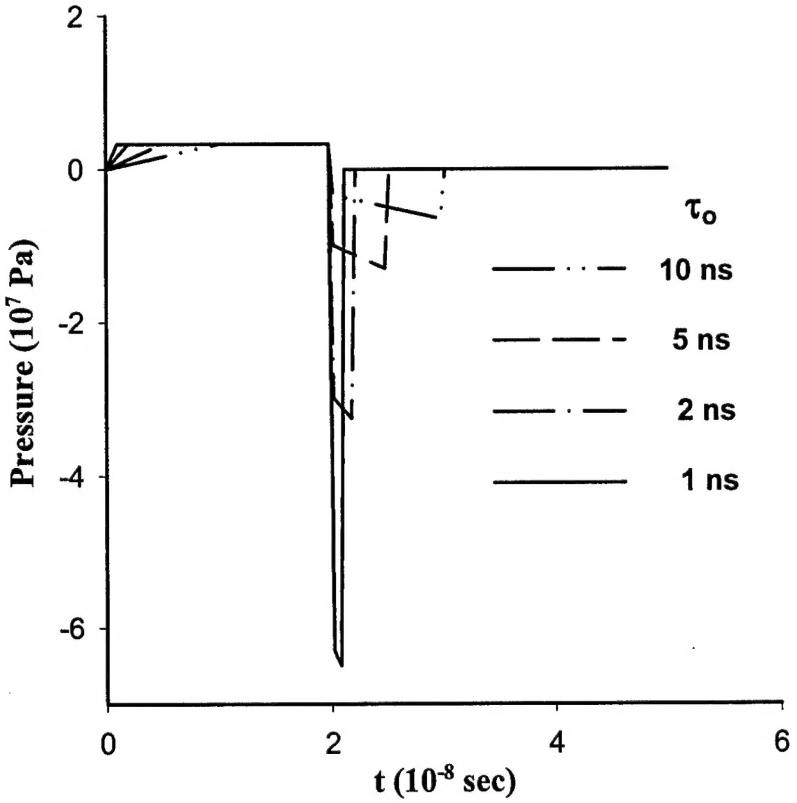

Figure 2

11.3 Full Non-Linear Treatment: Shock Waves, Vaporization, and Dangerous Chaotic Dynamics

The linearized, analytical treatment that we developed supplied important physical insight and produced the critical result concerning dangerous tensile stresses that will occur at the absorber's core even for low energy pulses. However, in order to analyze and predict the full range of thermodynamic and hydrodynamic responses in the absorber and the medium for any strength laser pulse, it is necessary to relax the condition that the medium would undergo only small changes in density. Relaxing this condition means that all physical responses can be investigated, such as shock waves and vaporization. However, it also means that the system is no longer mathematically linearizable, and the beauty of the analytical solution is replaced by the perseverance of a numerical solution.

In order to be able to predict the shock waves and vaporization generated in the medium from any laser pulse, the simplified EOS of Eq. (4) has to be abandoned for the medium and replaced by a more complete treatment that carefully represents variations in all thermodynamic properties: pressure, volume, temperature, entropy. This information is available for water from NBS Steam Tables. The information contained in the Steam Tables has to be carefully adapted for use in our investigation. For this work we had modify the NBS fitting algorithm in order to cover the vast range of values relevant to the liquid phase, the steam phase, and the fluid phase

above the critical point T_c. Our fitting algorithm is incorporated into our hydrodynamic computer code and produces the appropriate values of pressure and temperature from a given pair of values of specific volume and entropy. The region inside the vaporization dome in a pressure-volume representation is interpreted as an equilibrium mixture of vapor and liquid and a Van der Waals construction isused in this region. For all computer runs with this full EOS, the initial specific volume and entropy are chosen to correspond to the pre-laser temperature and pressure.

This EOS information allows us to write the energy conservation of Eq. (7) for the non-absorbing medium as

$$T\dot{s} = \frac{\lambda}{\rho}\nabla_u^2 T \tag{13}$$

Though fairly simple in appearance, Eq. (13) is absolutely crucial for the full analysis of all observable thermodynamic and hydrodynamic effects (P,V,T) that occur in response to energy absorption by the absorber.

With Eq. (13) and a full EOS for the medium, a complete treatment that predicts all thermodynamic and hydrodynamic responses is possible. Reliable predictions required careful implementation of a non-linear numerical algorithm. The numerical algorithm we chose was designed to optimize numerical stability but prevent unphysical numerical diffusion. Numerical stability is most easily obtained with low order algorithms, but they often introduce diffusion that is purely a numerical artifact with no physical basis. This numerical diffusion causes a smearing out of pressure fronts and limits the ability to model sharp shock fronts. In order to model a sharp shock front, a high order algorithm is needed. Unfortunately, a high order algorithm will generate unphysical numerical oscillations in the pressure front which limits the precision with which we can calculated the strength and speed of the shock front. In order to avoid both the unphysical smearing and the oscillations, we implemented a second order leap frog algorithm and incorporated a non-linear procedure called flux corrected transport, FCT.

The leap-frog method consists of evaluating at time t the acceleration $\ddot{u}$ of the mass points from the spatial derivative of pressure P at t from Eq. (3). This value of $\ddot{u}$ at t is then used to update the velocity $\dot{u}$ of the mass points during an increment of time Δt. However, the updating of $\dot{u}$ occurs from $t-\Delta t/2$ to new values at $t+\Delta t/2$; hence the name "leap-frog". The new values of $\dot{u}$ at $t+\Delta t/2$ at different spatial locations are then used to calculate the spatial derivatives and time derivatives of other quantities such as specific volume v ($1/\Delta$), and so on. The result is a cycle of updating every quantity by a time step of size Δt, with some quantities calculated at t_i and others calculated at $t_i+\Delta t/2$. Using this leap-frog method, numerical errors are reduced because they occur only as second order corrections or higher.

This higher order treatment can introduce unphysical numerical oscillations in quantities such as the pressure as seen in Fig. 3. In order to prevent these oscillations we must average them out by introducing numerical diffusion. However, if not done properly, adding this numerical diffusion can have the disadvantage of smearing out the shock fronts so that they are no longer sharp. FCT is a non-linear procedure that prevents oscillation but maintains sharp shock fronts. The FCT implementation is applied specifically to the velocity $\dot{u}$. It consists of two steps:

1)A zero-order diffusive flux with a weighting of 1/8 is added to $\dot{u}$ (r) from contributions from spatial neighbors, giving a diffused velocity $\dot{u}(r)^d$. This stabilizes the high order algorithm and

removes numerical oscillations (but unfortunately tends to smear out shock fronts).

$$\dot{u}(r)^{d}_{t+\Delta t/2} = \frac{3}{4}\dot{u}(r)_{t-\Delta t/2} + \frac{1}{8}\left[\dot{u}(r+\Delta r)_{t-\Delta t/2} + \dot{u}(r-\Delta r)_{t-\Delta t/2}\right] + \ddot{u}(r)_{t}\,\Delta t \qquad (14)$$

2)In order to resharpen the shock fronts without reintroducing the oscillations, the new velocity $\dot{u}$ (r) is obtained from the diffused velocity by applying a non-linear antidiffusion procedure defined by

$$\dot{u}(r)_{t+\Delta t/2} = \dot{u}(r)^{d}_{t+\Delta t/2} + f(r-\Delta r/2)^{c} - f(r+\Delta r/2)^{c} \qquad (15)$$

where the corrected flux is defined through

$$f(r+)r/2)^{c} = S\cong\max[0,\min(\mathrm{abs}(\mathrm{f(r+)r/2})),8S\ \mathrm{f(r+)r/2}),\ 8S\ \mathrm{f(r-)r/2}))] \qquad (16a)$$

with

$$f(r+\Delta r/2) = \frac{1}{8}\left[\dot{u}(r+\Delta r)^{d}_{t+\Delta t/2} - \dot{u}(r-\Delta r)^{d}_{t+\Delta t/2}\right] \qquad (16b)$$

and

$$S = \mathrm{sgn[f(r+)r/2)]} \qquad (16c)$$

The extended details of this non-linear numerical algorithm are given in the Journal of Applied Physics paper that is referenced above. The various numerical treatments are shown in Fig. 3, which also displays the success of the combined Leap-Frog, FCT algorithm for modeling sharp shock fronts.

Figure 3

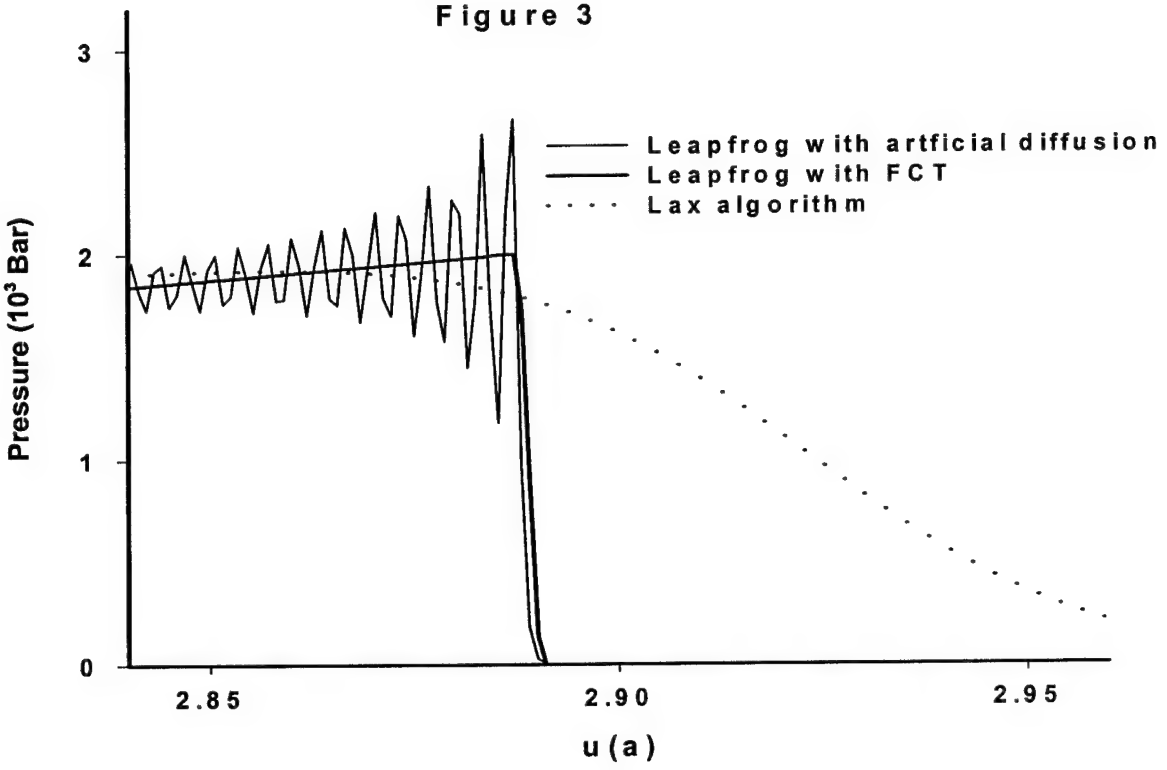

With the implementation of this flux corrected, leapfrog algorithm, our non-linear treatment allows us to calculate the full response of the system to laser pulses of any duration. An important aspect of this work is that both shock fronts and vaporization phase changes are calculated in unison from a first principles treatment of the system with no physical constraints that would limit the validity of the treatment. This is shown in Fig. 4. The propagation of a shock wave out into the medium at various times after absorption by a 1 :m size absorber of a 0.1 ns laser pulse is displayed in Fig. 4a. The expansion in the medium of the bubble produced from the same laser pulse is shown in Fig. 4b.

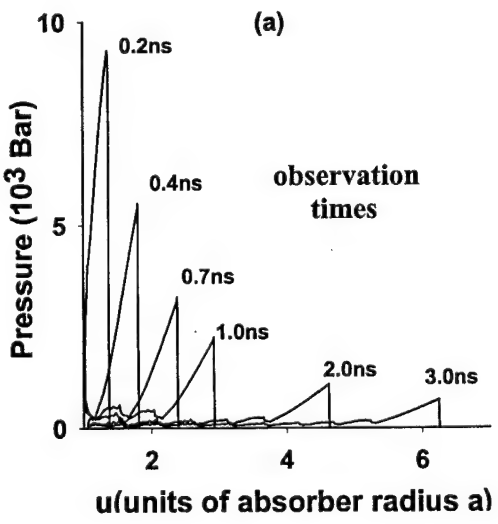

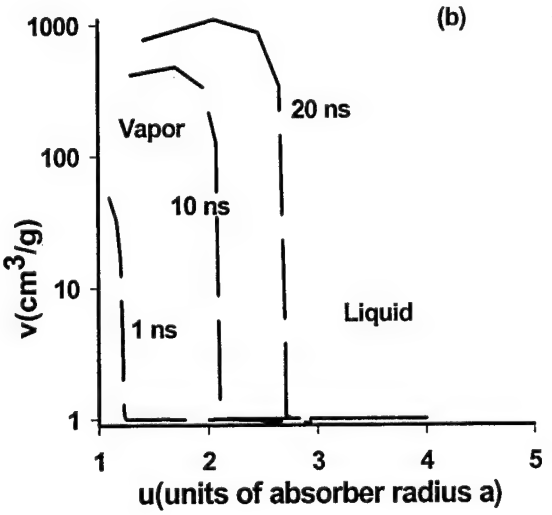

Figure 4

In order to get numerical results such as those of Fig. 4, input information is required about the properties of the absorber and the medium. The data for the medium was the P,V,T,S tables of water adapted from the NBS Steam Tables. For the case in which the absorbing particle is a melanosome we used a radius of a=1 :m, a density of Δ_o=1.35 g/cm^3, a specific heat of c_v=2.51 J/g≅K, a thermal conductivity of 8=5.56x10^{-3} J/cm≅K≅sec, and an absorption coefficient of $\forall_L$=10,000 cm^{-1}. The fluence of the laser pulse used was I_o=3.5 J/cm^2. In addition to these properties, Eqs. (4), (6), and (8) show that the bulk modulus B and thermal expansion coefficient $\forall$ of the absorber are also crucial parameters in the calculations. Unfortunately, measurements of these parameters have not been made for melanosomes and other microparticles. Experimental measurements of these parameters must be performed in order to allow the theoretical models to make accurate predictions of laser damage. The small size of the particles makes these measurements difficult but this model presents new suggestions for measuring these quantities, which have already been discussed in Section 11.2, just after Fig. 1. In order to show the capabilities of the model, we performed the calculations using graphite as a substitute for a melanosome based upon some chemical similarity and set B=39.4 GPa and $\forall$=2.98x10^{-5} K^{-1}. Figure 4a shows the capability of the model to display sharp shock fronts and the decay as it propagates outward from the absorber. Figure 4b shows the capability of the model to show the generation and expansion of a vapor bubble around the absorber.

Figures 5, 6, 7, 8, 9 show how the strength of the shock wave and bubble size depend on the laser fluence, melanosome thermal expansion coefficient, and melanosome bulk modulus, respectively. These figures emphasize the importance of obtaining accurate values for the thermo-mechanical properties of the absorber. An important part of the proposed work is to obtain these values for melanosomes and other absorbing particles, as described later.

Figure 5a shows the decay in the strength of the pressure jump of the leading shock front as the shock front propagates away from the absorber out into the medium. Information of this type is crucial in determining the likelihood of damage due to the shock front generated by a laser pulse since it allows the evaluation of whether or not the mechanical tolerances of the surrounding material will be exceeded, whether it be a polymer or biological cellular structures. Fg. 5b displays the non-linearity of the absorber-medium system's response to a laser pulse. To generate Fig. 5b, each curve in Fig. 5a has been scaled inversely to its fluence. If the system's response was to create a shock front that was linearly dependent on the laser fluence then the curves of Fig. 5b would be identical, which they are not. In Fig. 5, the absorbing particle is given the properties of a melanosome and the medium is water as in Fig. 4, but the same figure can be calculated for an absorber with any properties.

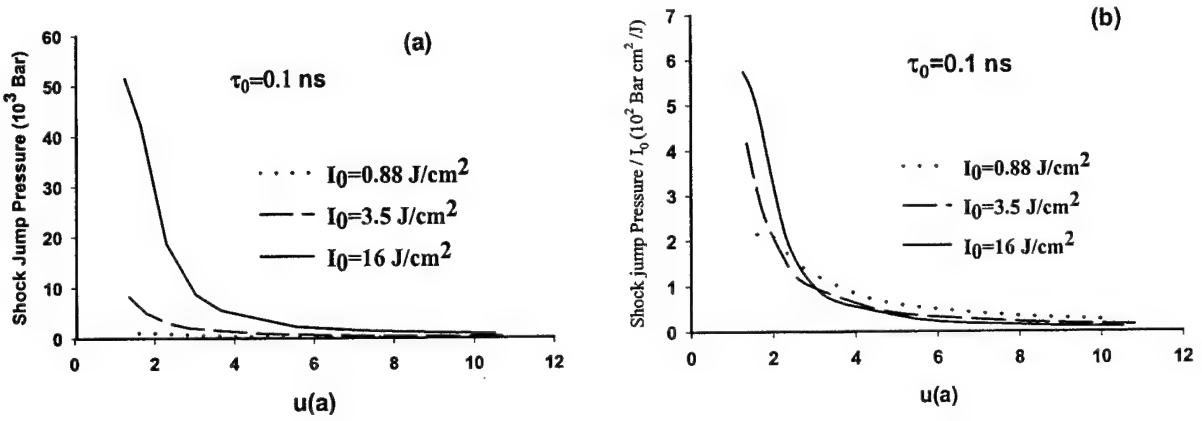
(a)
τ_0=0.1 ns
I_0=0.88 J/cm^2
I_0=3.5 J/cm^2
I_0=16 J/cm^2
Shock Jump Pressure (10^3 Bar)
u(a)
(b)
τ_0=0.1 ns
I_0=0.88 J/cm^2
I_0=3.5 J/cm^2
I_0=16 J/cm^2
Shock jump Pressure / I_0 (10^2 Bar cm^2 /J)
u(a)

Figure 5

Figure 6 displays the growth of the bubble from the surface of the absorbing particle into the surrounding medium for different fluences. The spherical bubble starts at the surface of the absorber at R=a(=1 :m) and expands outward. Fig. 6 plots the growing radius R(t) of the bubble as a function of time for a laser pulse of duration ϑ_o= 0.1 nsec. The properties of the particle and the medium are those of Figs. 4 and 5 but the fluence is lowered to examine the threshold region for bubble formation. In order to be detectable as a bubble, the vapor shell around the absorber must have sufficiently different optical properties from the enclosed absorbing particle. If we assume that this requires a vapor shell that must be at least 0.2 :m in thickness (R>1.2 :m), then the threshold fluence for bubble formation around a melanosome is 0.11 J/cm^2 which corresponds to a temperature rise of the melanosome of)T=174 K from the initial T_o =310 K (body temperature).

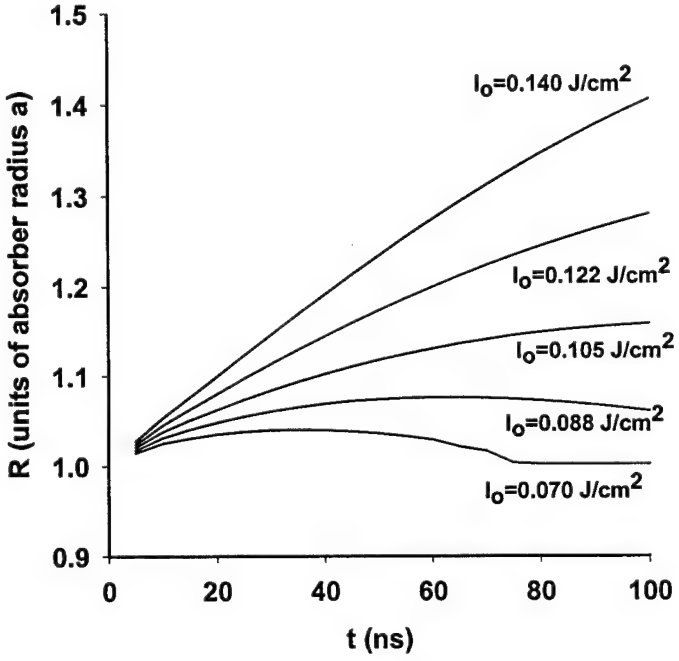

Figure 6

Figure 7 shows that the strength of the leading shockfront in the surrounding medium depends strongly on the thermal expansion coefficient $\forall$ of the absorbing particle, as expected. The laser pulse duration is ϑ_o=0.1 nsec and the fluence is I_o=0.88 J/cm^2. The lowest curve in this figure uses $\forall$=2.98x10^{-5} K^{-1} (graphite) and is identical to the lowest curve in Fig. 5a. However, as this figure shows, if an absorber is used with a larger value of $\forall$ then the resulting shockfront will be significantly larger and potentially much more damaging. Figure 7 emphasizes the necessity of knowing, or obtaining, accurate values of the thermo-mechanical properties of the absorber in order to be able to make accurate predictions of the physical response and potential for damage to the medium.

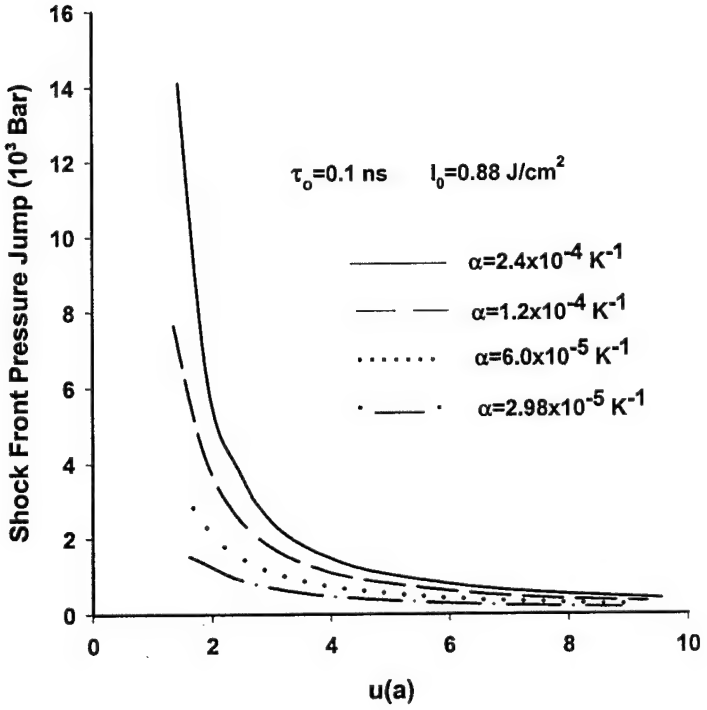

Figure 7

Figure 8 shows that the growth of the vapor bubble around the absorber also depends on the thermal expansion coefficient $\forall$. This is an unexpected result because it was previously assumed that bubble formation and growth depended only on the heat conducted into the medium. Figure 8 shows that surprisingly this is not true and that the mechanical pulsating of the absorber also affects the formation and growth of the bubble. Therefore, absorbers that undergo larger pulsations will produce larger bubbles. As with Fig. 7, this again shows that in order to predict the physical response of the system and to make realistic damage assessments, it is crucial to obtain accurate values of the thermo-mechanical properties of the absorber, which we propose to do.

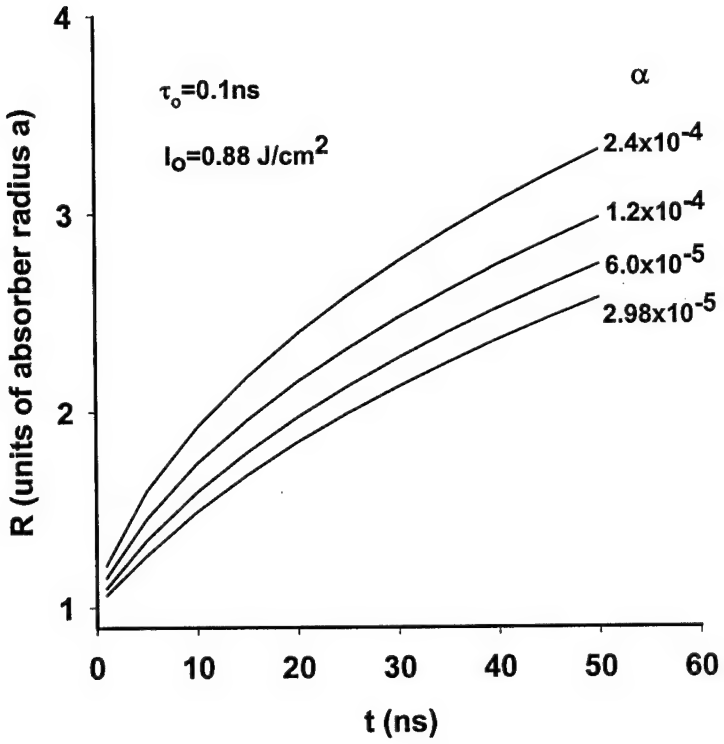

Figure 8

Figure 9 shows that the shockfront also depends on the absorber's bulk modulus B. The non-linearities in the governing equations when solved numerically as previously described produce the dependence displayed in Fig. 9. The strength of the shockfront at a distance of 1:m outside the surface of an absorber of radius a=1:m is plotted as a function of B for laser pulses of two different durations but both of the same fluence I_o=0.12 J/cm^2. The thermal expansion coefficient of the absorber is set to $\forall$=2.4x10^{-4} K^{-1}. The shorter the pulse duration, the greater the effect on the pressure generation for absorbers of different B.

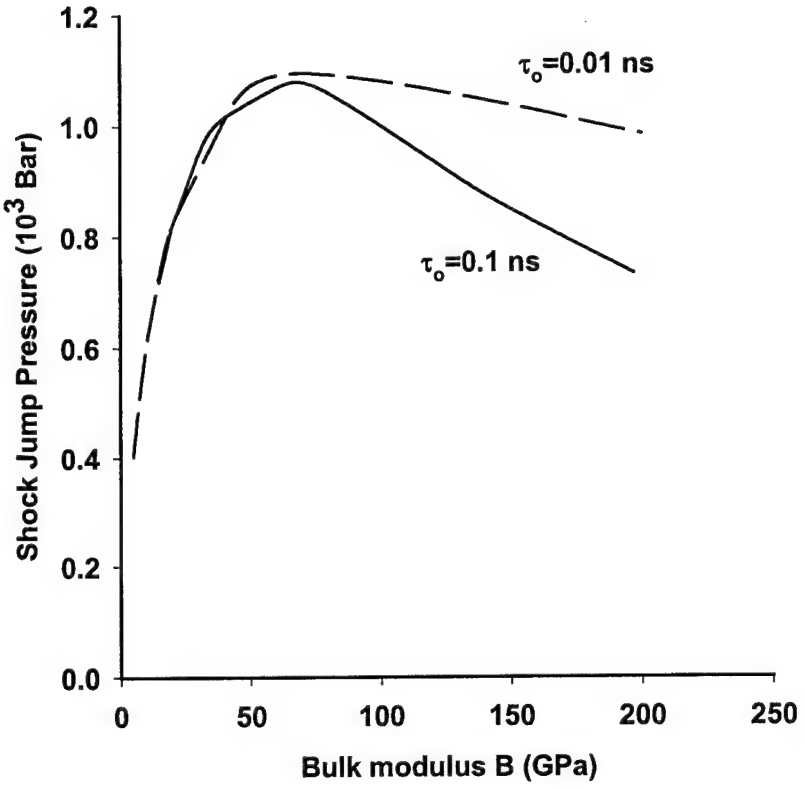

Figure 9

In addition to the above results, recent investigations uncovered an important surprise. Though the system appears simple, a spherical absorber in a transparent medium, the underlying physics is highly non-linear. We have found that this system displays chaotic dynamics, which may have major implications for damage and safety considerations. Figure 10 displays the pressure signal as a function of time at a location in the medium that is 4a from the center of the absorber. For this figure, the laser pulse had a duration of ϑ_o=1.0 nsec and a fluence of I_o= 0.14 J/cm^2. It can be seen that at approximately 77 nsec after the laser pulse, the pressure oscillations in the medium undergo a spontaneous change in frequency. More importantly, the pressure oscillations which had been decreasing in strength, spontaneously increase dramatically in strength. These spontaneous fluctuations may result in much greater damage from the laser pulse than otherwise expected. The investigation and prediction of this chaotic behavior is only possible with the present model which analyzes the dynamics in terms of the underlying thermodynamic physics of the laser-matter interactions.

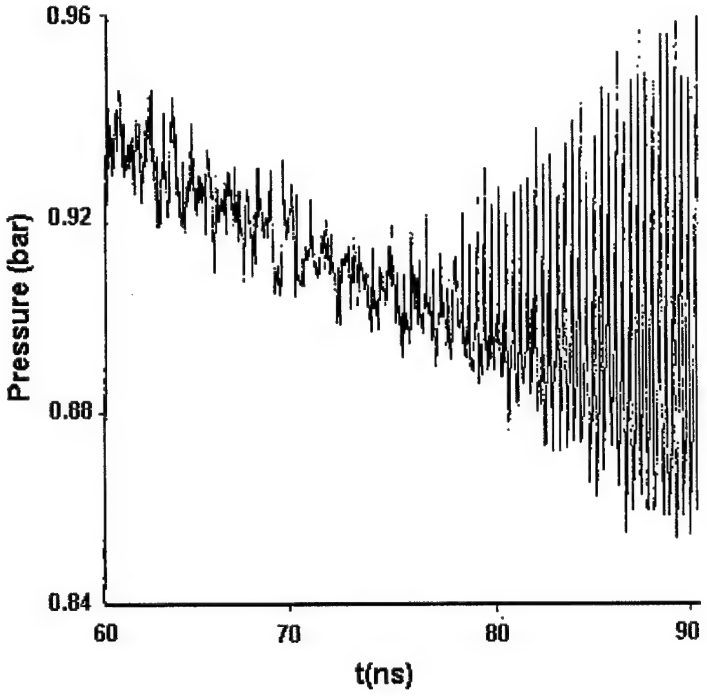

Figure 10

Figure 11 is the power spectrum of the pressure signal of Fig. 10, examined specifically at t=65 nsec. At earlier times, soon after the laser pulse, the pressure oscillations occur predominantly at the natural frequency of the system, f_c=1/ϑ_c. However, by 65 nsec, Fig. 11 shows that the pressure signal has evolved by a series of subharmonic bifurcations into chaotic turbulence. The dominant frequency at this later time is the 1/9 subharmonic of f_c. To our knowledge, the various subharmonics displayed in Fig. 11 have not been reported for other

systems. This may be evidence of new routes to chaos and has important implications for research in non-linear physics.

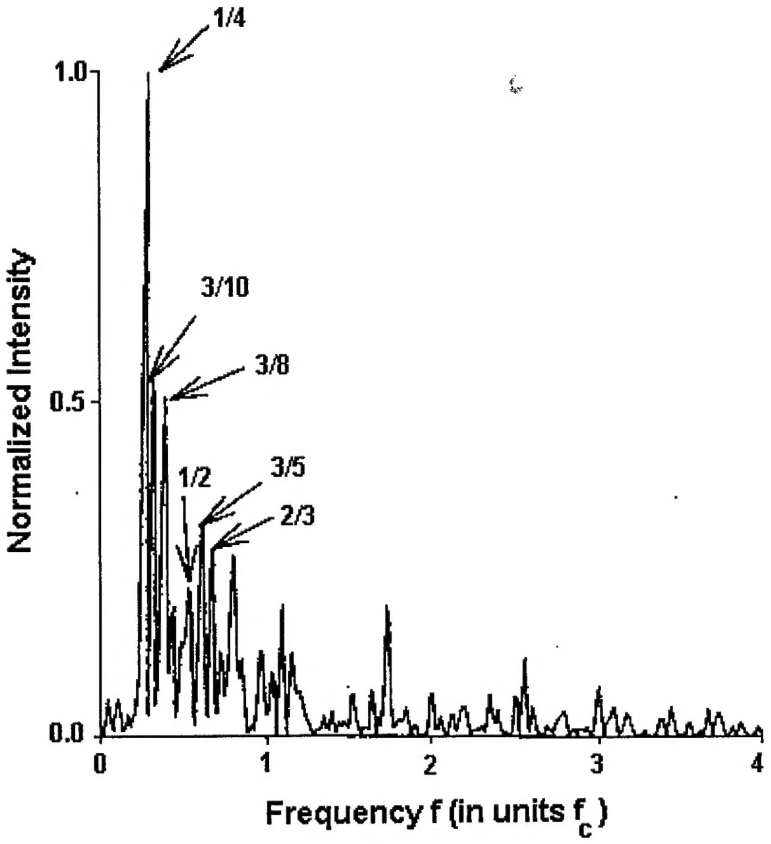

Figure 11

Figure 12 displays a grey-scale dynamical power spectrum that shows how the dominant Fourier frequency components of the pressure response shifts in time. The observation time in Fig. 12 starts with the 1.0 nsec laser pulse and continues for 100 nsec.

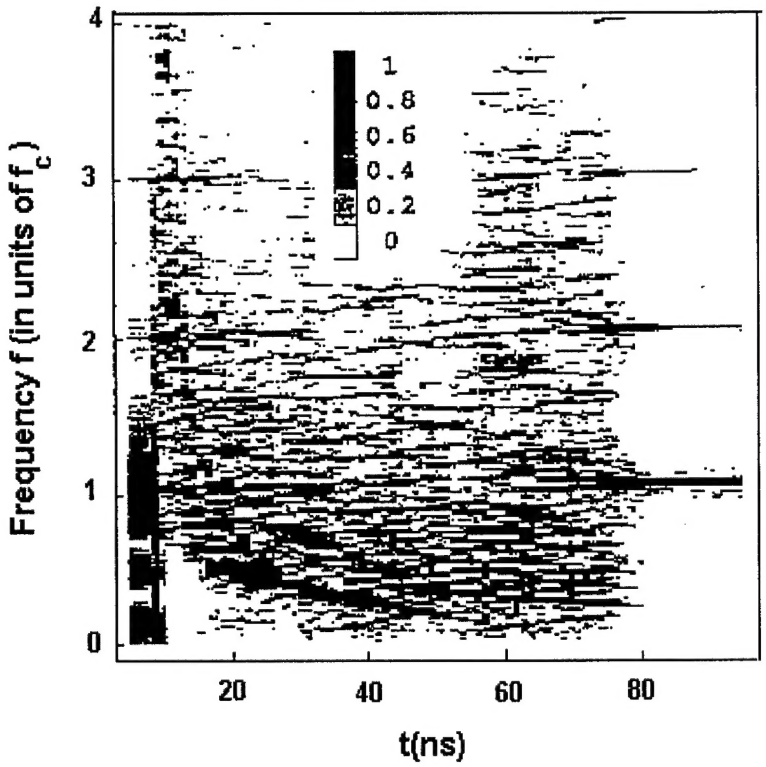

Figure 12

Finally, Fig. 13 shows that the behavior of the system is extremely complex. Figure 13 has similar conditions to those of Fig. 10 except that the duration of the laser pulse in Fig. 13 is ϑ_o=10 nsec and the fluence is 0.088 J/cm^2. This system also displays spontaneous jumps in the frequency and strength of the pressure oscillations, but in an opposite manner to those of Fig. 10. Here in Fig. 13, the system spontaneously switches to weaker and slower oscillations, whereas in Fig. 10 the behavior spontaneously switched to stronger and higher frequency oscillations. This may imply that some laser pulse durations and fluences may cause large collateral damage, as in Fig. 10, whereas other laser pulses may cause significantly less collateral damage, as in Fig. 13. The investigation of these possibilities is now starting.

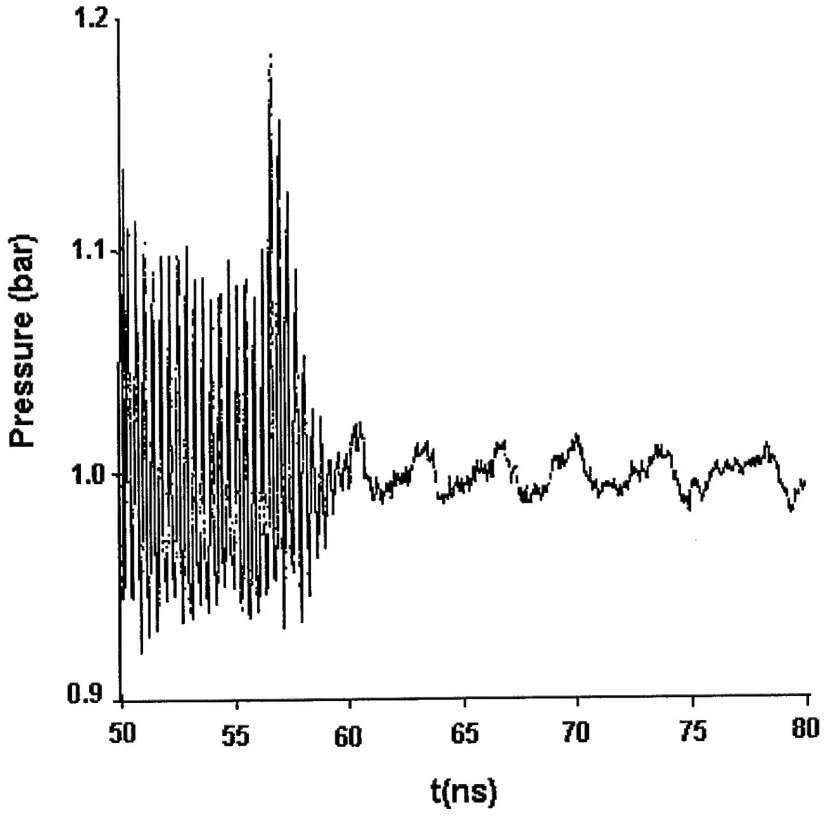

Figure 13

11.4 Summary

The theoretical and computational model developed is the most comprehensive model for investigating the effects and potential risk for damage of laser pulses on transparent materials containing strongly absorbing particles. The treatment is based upon the fundamental physical principles governing the behavior of matter and is therefore applicable to a variety of materials

such as the biological tissue of the retina, polymers and dielectric electronics, and other micro and nano particles. A variety of unexpected effects have been discovered and quantified.

Our work established the unexpected result that the tensile stress at the core of the absorber continues to grow even as the laser pulse duration was made shorter than the acoustic transit time. The fact that it is the tensile, negative pressure that continues to increase at the core makes the situation especially dangerous. It shows that the same energy delivered in a shorter pulse is increasingly more likely to cause an absorbing particle to explode like a laser-activated handgrenade. Our work shows that this dangerous effect will be present not just for melanosomes in the retina, but for any absorbing particle in any media, and for self-focusing in transparent uniform materials such as water or polymers. This discovery implies that laser pulses become increasingly more dangerous as the pulse length is shortened and that the continual increase in tensile stress can cause the absorber to explode at increasingly lower laser energies.

We have discovered that the growth of the vapor bubble around the absorber also depends on the thermal expansion coefficient $\forall$. This is an unexpected result because it was previously assumed that bubble formation and growth depended only on the heat conducted into the medium. Instead, the mechanical pulsating of the absorber also affects the formation and growth of the bubble. Therefore, absorbers that undergo larger pulsations will produce larger bubbles. The dependence of shock wave strength and bubble size on the B and $\forall$ of the absorber implies that precise predictions of the physical response of the system and the potential for damage to the medium can only be achieved once there is accurate information about these mechanical properties of the absorbing particle. These properties are not known for melanosomes or many other microparticles that are present in electronic, polymeric and other technologically important materials. In our work, we have chosen specific values in order to be able to display the power of our model and elucidate the general pattern of the dynamics expected for a range of similar systems. The small size of these particles makes the measurements extremely difficult. However, the work described here has shown how measurements of the pressure transients in the surrounding medium can be used to determine these properties.

In addition to the above results, our investigations uncovered an important surprise. Though the system appears simple, a spherical absorber in a transparent medium, the underlying physics is highly non-linear. We have found that this system displays chaotic dynamics, which may have major implications for damage and safety considerations. Sudden spontaneous fluctuations may result in much greater damage from the laser pulse than otherwise expected. Some laser pulse durations and fluences may cause large collateral damage, as in Fig. 10, whereas other laser pulses may cause significantly less collateral damage, as in Fig. 13. The investigation and prediction of this chaotic behavior is only possible with the present model which analyzes the dynamics in terms of the underlying thermodynamic physics of the laser-matter interactions.

12. Transitions